JACS
JOURNAL OF THE AMERICAN CHEMICAL SOCIETY
Communication
pubs.acs.org/JACS

Crystal Structure of Selenolate-Protected $Au_{24}(SeR)_{20}$ Nanocluster

Yongbo Song, Shuxin Wang, Jun Zhang, Xi Kang, Shuang Chen, Peng Li, Hongting Sheng, and Manzhou Zhu*

Department of Chemistry, Anhui University, Hefei, Anhui 230601, P. R. China

Supporting Information

ABSTRACT: We report the X-ray structure of a selenolate-capped $Au_{24}(SeR)_{20}$ nanocluster (R = C_6H_5). It exhibits a prolate Au_8 kernel, which can be viewed as two tetrahedral Au_4 units cross-joined together without sharing any Au atoms. The kernel is protected by two trimeric $Au_3(SeR)_4$ staple-like motifs as well as two pentameric $Au_5(SeR)_6$ staple motifs. Compared to the reported gold–thiolate nanocluster structures, the features of the Au_8 kernel and pentameric $Au_5(SeR)_6$ staple motif are unprecedented and provide a structural basis for understanding the gold–selenolate nanoclusters.

Thiolate-stabilized gold nanoclusters have attracted wide research interest in recent years. To date, a number of size-discrete gold nanoclusters have been identified,[1−14] and a few of them have been structurally characterized by single-crystal X-ray crystallography.[15−23] In parallel with the thiolate-protected gold nanoclusters, recent works have revealed that, by changing the ligand of the gold nanoclusters from thiolate to selenolate (HSeR), more-stable gold nanoclusters can be produced, and the related properties have been studied.[24−27] These studies also found that selenolate-protected $Au_n(SeR)_m$ nanoclusters possess characteristics different from those of the $Au_n(SR)_m$ counterparts and thus have considerable potential as new functional nanomaterials. However, there have been no reports thus far on the successful crystallization of $Au_n(SeR)_m$ nanoclusters. In order to clarify the precise correlation between the ligand and cluster stability, the structure of nanoclusters protected by selenolate should be pursued. Herein we report the first structure of selenolate-stabilized $Au_{24}(SeC_6H_5)_{20}$ nanoclusters.

Details of the synthesis are provided in the Supporting Information. Briefly, $HAuCl_4{\cdot}3H_2O$ was dissolved in water and then phase-transferred to CH_2Cl_2 with the aid of tetraoctylammonium bromide (TOAB). Then, both C_6H_5SeH and $NaBH_4$ were added simultaneously to convert Au(III) into Au(I) or Au(0) by co-reduction. After reaction overnight, the aqueous phase was removed. The mixture in the organic phase was rotavaporated, and then washed several times with CH_3OH/hexane. Dark brown crystals were crystallized from CH_2Cl_2/ethanol over 2−3 days. The crystals were then collected. The structure of $Au_{24}(SeC_6H_5)_{20}$ was determined by X-ray crystallography. The optical absorption spectrum of $Au_{24}(SeC_6H_5)_{20}$ nanoclusters (dissolved in toluene or CH_2Cl_2) shows three stepwise peaks at 380, 530, and 620 nm (Figure 1). Of note, the optical spectrum of the thiolate counterpart, i.e., $Au_{24}(SC_2H_4Ph)_{20}$ nanoclusters (dissolved in toluene or CH_2Cl_2), shows a distinct band at 765 nm and a shoulder band at 400 nm.[28]

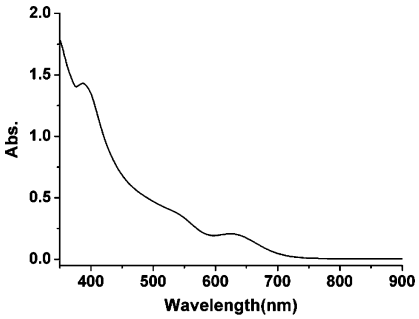

Figure 1. Optical absorption spectrum of $Au_{24}(SeC_6H_5)_{20}$ nanoclusters.

The total structure of the $Au_{24}(SeC_6H_5)_{20}$ nanocluster is shown in Figure 2. A similar structure was discussed in previous DFT calculations by Pei et al. on thiolate-capped $Au_{24}(SR)_{20}$ nanoclusters.[29] To find out details of the atom-packing structure, we focus on the $Au_{24}Se_{20}$ framework without the carbon tails (Figure 3A). The $Au_{24}Se_{20}$ can be divided into a prolate Au_8 kernel (Figure 3A, highlighted in green), two trimeric Au_3Se_4 staple-like motifs (Figure 3B, labeled i and highlighted with blue curves), and two pentameric Au_5Se_6 staple motifs (Figure 3B, labeled ii and highlighted with blue curves). Following this anatomy, the $Au_{24}Se_{20}$ framework can

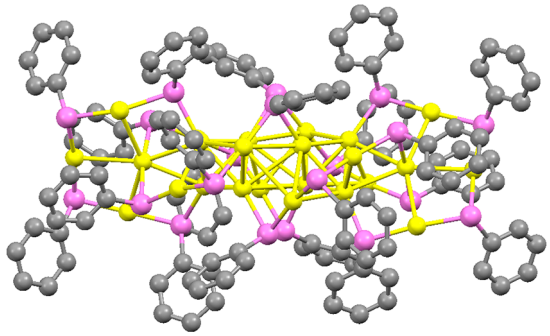

Figure 2. Crystal structure of a selenophenol-protected $Au_{24}(SeC_6H_5)_{20}$ nanocluster. (Color labels: yellow = Au, violet = Se, gray = C; all H atoms are not shown).

Received: December 25, 2013
Published: February 18, 2014

   dx.doi.org/10.1021/ja4131142 | J. Am. Chem. Soc. 2014, 136, 2963−2965

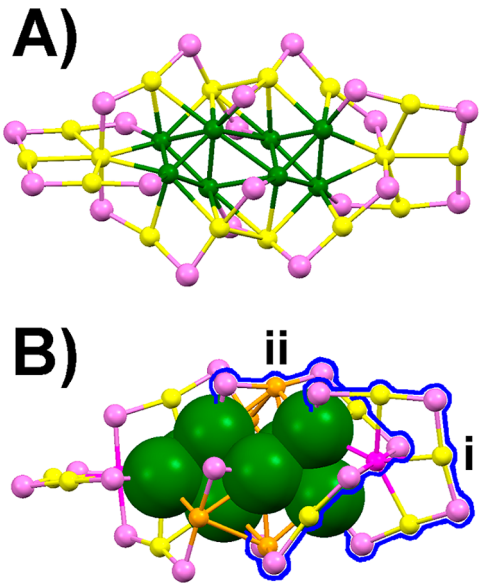

Figure 3. (A) $Au_{24}Se_{20}$ framework with the prolate Au_8 kernel highlighted in green. (B) Selenolate-binding motifs in $Au_{24}Se_{20}$: (i) $Au_3(SeR)_4$ staple and (ii) $Au_5(SeR)_6$ staple. (Color labels: green/yellow, orange, magenta = kernel/surface Au atoms, violet = Se).

be written as $Au_8[Au_3Se_4]_2[Au_5Se_6]_2$. The entire structure of $Au_{24}Se_{20}$ is like a butterfly (Figure 3A).

For a more detailed anatomy of the total structure, we start with the prolate Au_8 kernel (Figure 4A,B), which may be viewed as two tetrahedral Au_4 units cross-joined together without sharing any Au atoms. The prolate Au_8 kernel has never been observed previously but only discussed in DFT calculations on $Au_{20}(SR)_{16}$ and $Au_{24}(SR)_{20}$.[29,30] In either unit of the dimeric Au_8 kernel, the bond lengths range from 2.701 to 2.823 Å (average 2.735 Å). Compared with the theoretical Au_8 kernel (the best candidate structure predicted by Pei et al.[29]), the bond between Au(10) and Au(14) cannot be formed (see Figure S1), which indicates the distance between the Au_4 units is much farther. Furthermore, the two sets of Au−Au (Figure 4B, highlighted in green and yellow, respectively) are nearly in the same plane (the angle sum of quadrangle: 359.78° and 359.79°). From another perspective, there are two pairs of Au−Au (Figure 4C, highlighted in yellow), in which each Au atom is part of the pentameric Au_5Se_6 staple motifs. The Au_4 units are joined together via either pair of Au−Au, which could increase the stability of the Au_8 kernel. From the side view, the Au_{12} framework looks like a gold ingot (Figure 4D).

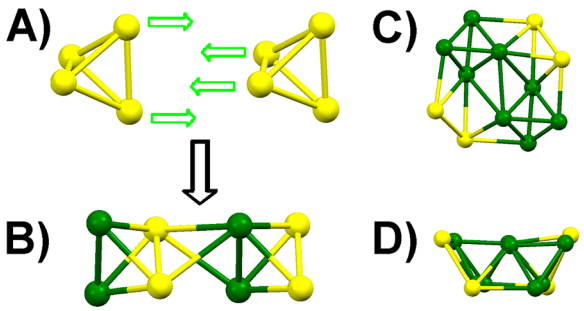

Figure 4. (A,B) Au_8 kernel structure in $Au_{24}(SeC_6H_5)_{20}$. (C) Top view and (D) side view of the Au_{12} framework containing the Au_8 kernel (highlighted in green) and other four Au atoms (highlighted in yellow).

As for the surface-protecting motifs in $Au_{24}(SeC_6H_5)_{20}$, we start with the two pentameric Au_5Se_6 staples, which are linked with the middle of the Au_8 kernel (Figure 3A). It is worth noting that the pentameric (Au_5Se_6) staple is indeed for the first time observed experimentally, even in the thiolate-capped gold nanoclusters. Such a pentameric staple was predicted to exist in earlier theoretical works[29] in the structure of the experimentally identified $Au_{24}(SR)_{20}$.[28] In the Au_5Se_6 staple, the bond angles of (R)Se−Au−Se(R) range from 163.80° to 175.97° (nearly in straight line), and the average Au−Se bond length is 2.426 Å. Furthermore, the trimeric staple motifs, which are linked with the ends of the Au_8 kernel (Figure 3A), have been reported by Jin et al. in the structure $Au_{23}(SC_6H_{11})_{16}$.[15] Compared with the trimeric $Au_3(SR)_4$ motif, the bond length of Au−Se (average: 2.427 Å) is longer than that of Au−S (average: 2.301 Å), which is due to the larger selenium atom than the suldur atom (covalent radius of selenium r = 1.20 Å versus sulfur atom r = 1.05 Å). Interestingly, the two Au_5Se_6 staple motifs are combined by two pairs of Au−Au bonds (Figure 3B, highlighted in orange), and the Au−Au bonds are 3.091 and 3.077 Å, respectively. In addition, the trimeric Au_3Se_4 staple motifs are closely linked with the pentameric staple through the Au−Au bond (Figure 3B, highlighted in magenta), with the average Au−Au bond length being 2.986 Å. This particular configuration between the stable motifs makes the structure more stable.

In summary, this work reports the first crystal structure of a selenolate-capped $Au_{24}(SeR)_{20}$ nanocluster. This nanocluster features a new type of Au_5Se_6 staple motif and a prolate Au_8 kernel, which will offer new perspectives in understanding the atomic structure and growth of gold−selenolate nanoclusters. The results will also provide an opportunity for understanding the selenolate-protected Au nanoclusters and comparing with the thiolate-protected counterparts.

■ ASSOCIATED CONTENT

Supporting Information

Detailed information about the synthesis, X-ray analysis of $Au_{24}(SeC_6H_5)_{20}$, and Figure S1. This material is available free of charge via the Internet at http://pubs.acs.org.

■ AUTHOR INFORMATION

Corresponding Author

zmz@ahu.edu.cn

Notes

The authors declare no competing financial interest.

■ ACKNOWLEDGMENTS

We acknowledge financial support by NSFC (21072001, 21201005, 21372006), the Ministry of Education and Ministry of Human Resources and Social Security, the Education Department of Anhui Province, Anhui Province International Scientific and Technological Cooperation Project, and 211 Project of Anhui University.

■ REFERENCES

(1) Qian, H.; Zhu, M.; Wu, Z.; Jin, R. *Acc. Chem. Res.* **2012**, *45*, 1470.
(2) Nishigaki, J.; Tsunoyama, R.; Tsunoyama, H.; Ichikuni, N.; Yamazoe, S.; Negishi, Y.; Ito, M.; Matsuo, T.; Tamao, K.; Tsukuda, T. *J. Am. Chem. Soc.* **2012**, *134*, 14295.

(3) Qian, H.; Zhu, Y.; Jin, R. *Proc. Natl. Acad. Sci. U.S.A.* **2012**, *109*, 696.
(4) Shibu, E. S.; Pradeep, T. *Chem. Mater.* **2011**, *23*, 989.
(5) Dass, A. *J. Am. Chem. Soc.* **2011**, *133*, 19259.
(6) Negishi, Y.; Kurashige, W.; Niihori, Y.; Iwasa, T.; Nobusada, K. *Phys. Chem. Chem. Phys.* **2010**, *12*, 6219.
(7) Qian, H.; Jiang, D.; Li, G.; Gayathri, C.; Das, A.; Gil, R. R.; Jin, R. *J. Am. Chem. Soc.* **2012**, *134*, 16159.
(8) (a) Shichibu, Y.; Negishi, Y.; Tsunoyama, H.; Kanehara, M.; Teranishi, T.; Tsukuda, T. *Small* **2007**, *3*, 835. (b) Yu, Y.; Luo, Z.; Yu, Y.; Lee, J. Y.; Xie, J. *ACS Nano* **2012**, *6*, 7920.
(9) Qian, H.; Zhu, Y.; Jin, R. *J. Am. Chem. Soc.* **2010**, *132*, 4583.
(10) Krommenhoek, P. J.; Wang, J.; Hentz, N.; Johnston-Peck, A. C.; Kozek, K. A.; Kalyuzhny, G.; Tracy, J. B. *ACS Nano* **2012**, *6*, 4903.
(11) Nimmala, P. R.; Yoon, B.; Whetten, R. L.; Landman, U.; Dass, A. *J. Phys. Chem. A* **2013**, *117*, 504.
(12) Qian, H.; Jin, R. *Chem. Mater.* **2011**, *23*, 2209.
(13) Negishi, Y.; Sakamoto, C.; Ohyama, T.; Tsukuda, T. *J. Phys. Chem. Lett.* **2012**, *3*, 1624.
(14) Tang, Z.; Robinson, D. A.; Bokossa, N.; Xu, B.; Wang, S.; Wang, G. *J. Am. Chem. Soc.* **2011**, *133*, 16037.
(15) Das, A.; Li, T.; Nobusada, K.; Zeng, C.; Rosi, N. L.; Jin, R. *J. Am. Chem. Soc.* **2013**, *135*, 18264.
(16) Jadzinsky, P. D.; Calero, G.; Ackerson, C. J.; Bushnell, D. A.; Kornberg, R. D. *Science* **2007**, *318*, 430.
(17) Heaven, M. W.; Dass, A.; White, P. S.; Holt, K. M.; Murray, R. W. *J. Am. Chem. Soc.* **2008**, *130*, 3754.
(18) Zhu, M.; Aikens, C. M.; Hollander, F. J.; Schatz, G. C.; Jin, R. *J. Am. Chem. Soc.* **2008**, *130*, 5883.
(19) Zhu, M.; Eckenhoff, W. T.; Pintauer, T.; Jin, R. *J. Phys. Chem. C* **2008**, *112*, 14221.
(20) Zeng, C.; Li, T.; Das, A.; Rosi, N. L.; Jin, R. *J. Am. Chem. Soc.* **2013**, *135*, 10011.
(21) Zeng, C.; Qian, H.; Li, T.; Li, G.; Rosi, N. L.; Yoon, B.; Barnett, R. N.; Whetten, R. L.; Landman, U.; Jin, R. *Angew. Chem., Int. Ed.* **2012**, *51*, 13114.
(22) Qian, H.; Eckenhoff, W. T.; Zhu, Y.; Pintauer, T.; Jin, R. *J. Am. Chem. Soc.* **2010**, *132*, 8280.
(23) Wan, X.; Lin, Z.; Wang, Q. *J. Am. Chem. Soc.* **2012**, *134*, 14750.
(24) Meng, X.; Xu, Q.; Wang, S.; Zhu, M. *Nanoscale* **2012**, *4*, 4161.
(25) Xu, Q.; Wang, S.; Liu, Z.; Xu, G.; Meng, X.; Zhu, M. *Nanoscale* **2013**, *5*, 1176.
(26) Kurashige, W.; Yamaguchi, M.; Nobusada, K.; Negishi, Y. *J. Phys. Chem. Lett.* **2012**, *3*, 2649.
(27) Kurashige, W.; Yamazoe, S.; Kanehira, K.; Tsukuda, T.; Negishi, Y. *J. Phys. Chem. Lett.* **2013**, *4*, 3181.
(28) Zhu, M.; Qian, H.; Jin, R. *J. Phys. Chem. Lett.* **2010**, *1*, 1003.
(29) Pei, Y.; Pal, R.; Liu, C.; Gao, Y.; Zhang, Z.; Zeng, X. *J. Am. Chem. Soc.* **2012**, *134*, 3015.
(30) Pei, Y.; Gao, Y.; Shao, N.; Zeng, X. *J. Am. Chem. Soc.* **2009**, *131*, 13619.